SUPPLEMENTAL INFORMATION

Figure S1. Properties of the translational efficiency score, related to Figure 1. (a-b) lincRNAs do not show substitution patterns consistent with protein-coding regions across mice. (a) The number of non-synonymous substitutions (dN) and the number of synonymous substitutions (dS) were computed from single nucleotide polymorphisms across 17 mouse strains (see **Methods**). The cumulative density distribution of the log of the dN/dS ratio is shown for the known protein-coding regions (blue) and for all ORFs in intronic regions (green) and lincRNAs (red). (b) The cumulative density distribution of the log of the dN/dS ratio is shown for the known protein-coding regions (blue) and for the ORF with the maximum ribosome occupancy for intronic regions (green) and lincRNAs (red). (c-f) Ribosome occupancy on 5'-UTRs and lincRNAs are not due to the presence of open-reading-frames. (c) The cumulative density distribution of the TE-mean across 3'-UTRs (gray), coding regions (purple), 5'-UTRs (light blue), 5'-UTRs excluding all AUG defined uORFs (dark blue), and 5'-UTRs excluding all uORFs defined by AUG, CUG, UUG, or GUG start codons. (d) The cumulative density distribution of the TE-max across 90 base windows for the 3'-UTRs (gray), coding regions (purple), 5'-UTRs (light blue), and 5'-UTRs excluding all uORFs (dark blue). (e) The cumulative density distribution of the TE-mean across 3'-UTRs (gray), coding regions (purple), lincRNA regions within an ORF (dark red), and lincRNA regions not containing an ORF (light red). (f) The cumulative density distribution of the TE-max across 90 base windows for the 3'-UTRs (gray), coding regions (purple), lincRNA regions within an ORF (dark red), and lincRNA regions not containing an ORF (light red).

Figure S2. Translational efficiency of the window with maximum ribosome protected density fails to separate translated and non-translated RNAs, related to Figure 2. To identify regions within transcripts that may be translated, we scanned 90-mer windows and identified the window with the maximum density of unique ribosome protected sites. For each of these maximum density windows, we computed the translational efficiency using only reads contained within the expected ribosome protected fragment length distribution (see **Methods**). The scatter plot of RNA expression (log scale, x-axis) compared to the translational efficiency of the maximum density 90-mer window (TE score, log scale, y-axis) for coding regions (purple dots), 3'-UTRs (gray dots), 5'-UTRs (blue dots), classical ncRNAs (black dots), and lincRNAs (red dots). Horizontal lines correspond to the 5^{th}, 25^{th}, 50^{th}, 75^{th}, and 95^{th} percentiles of the

translational efficiency score for protein-coding regions. The overlaid density distributions of the max-density TE scores for each feature class are shown. (b-c) The translational efficiency score calculated using non-polyA selected mRNA fails to separate coding and non-coding RNAs. (b) Cumulative distribution of the average translational efficiency score for the untreated ribosome fractions compared to non-polyA selected mRNA across coding regions (purple line), 3'-UTRs (gray line), 5'-UTRs (blue line), classical ncRNAs (black line), and lincRNAs (red line). (c) Cumulative distribution of the translational efficiency computed using the max 90-mer window across the same classes. (d-e) Ribosome occupancy at start codons, following treatment with harringtonine, does not separate translated and non-translated RNAs. Cumulative density distribution of the enrichment of harringtonine-treated samples at defined start codons for coding regions (purple), 3'-UTRs (gray), 5'-UTRs (blue), lincRNAs (red), and classical ncRNAs (black). Different harringtonine treatment times are shown (90s, 120s, 150s, and 180s). For coding regions of protein-coding mRNAs, the annotated start codon is used in all panels. For all other features, (d) shows the maximum peak identified over all putative ORFs in the transcript. (e) shows enrichment at the ORF relative to the highest ribosome occupancy in untreated conditions.

Figure S3. The ribosome release score robustly separates coding and non-coding RNAs, related to Figure 3. The RRS can also be computed by counting all reads that are fully contained within an ORF compared to its 3'-UTR (see **Methods**). This allows the RRS to be conservatively assigned to each ORF. (a) Scatter plot of the TE-mean score for each ORF (log scale, x-axis) compared to its ribosome release score (log scale, y-axis) for coding genes (purple), 5'-UTRs (blue), 3'-UTRs (gray), classical ncRNAs (black), and lincRNAs (red). For known coding regions, we show the annotated ORF and for all other features we computed all possible ORFs (see **Methods**). The TE-mean score reflects the mean over each ORF. The dashed lines represent the 95^{th} percentile of 3'-UTR values. Along each axis, all points are summarized using an overlaid density plot. (b) Cumulative density distribution of the RRS for the putative ORF with the highest ribosome occupancy (see **Methods**) for protein-coding regions (purple), 3'-UTRs (gray), 5'-UTRs (blue), classical ncRNAs (black), and lincRNAs (red). The dashed line indicates the fold difference between the median score for lincRNAs and protein-coding regions. (c) A cumulative density distribution of the maximum RRS over any ORF within a transcript (see **Methods**).

Figure S4. The ribosome release scores of lincRNAs are well separated from small coding genes, related to Figure 4. Cumulative density distribution of the RRS for lincRNAs defined across all ORFs (light red), lincRNAs defined by the ORF with the highest ribosome occupancy (dark red), small coding regions (light blue), and all coding regions (dark blue).

Supplemental Figure1

Click here to download Supplemental Figure: Guttman2013_SuppFigure1.pdf

Supplemental Figure 1

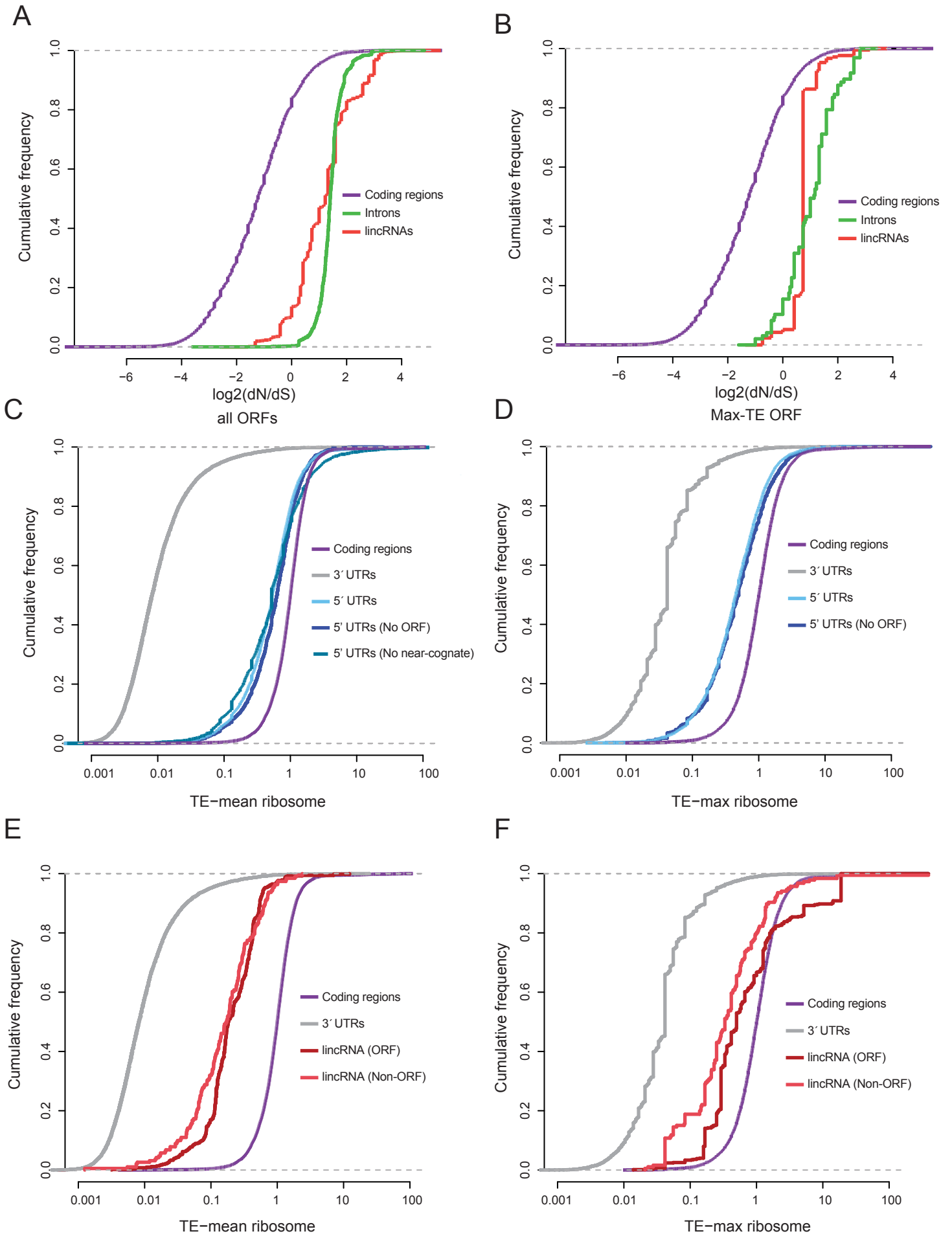

Supplemental Figure2

Click here to download Supplemental Figure: Guttman2013_SuppFigure2.pdf

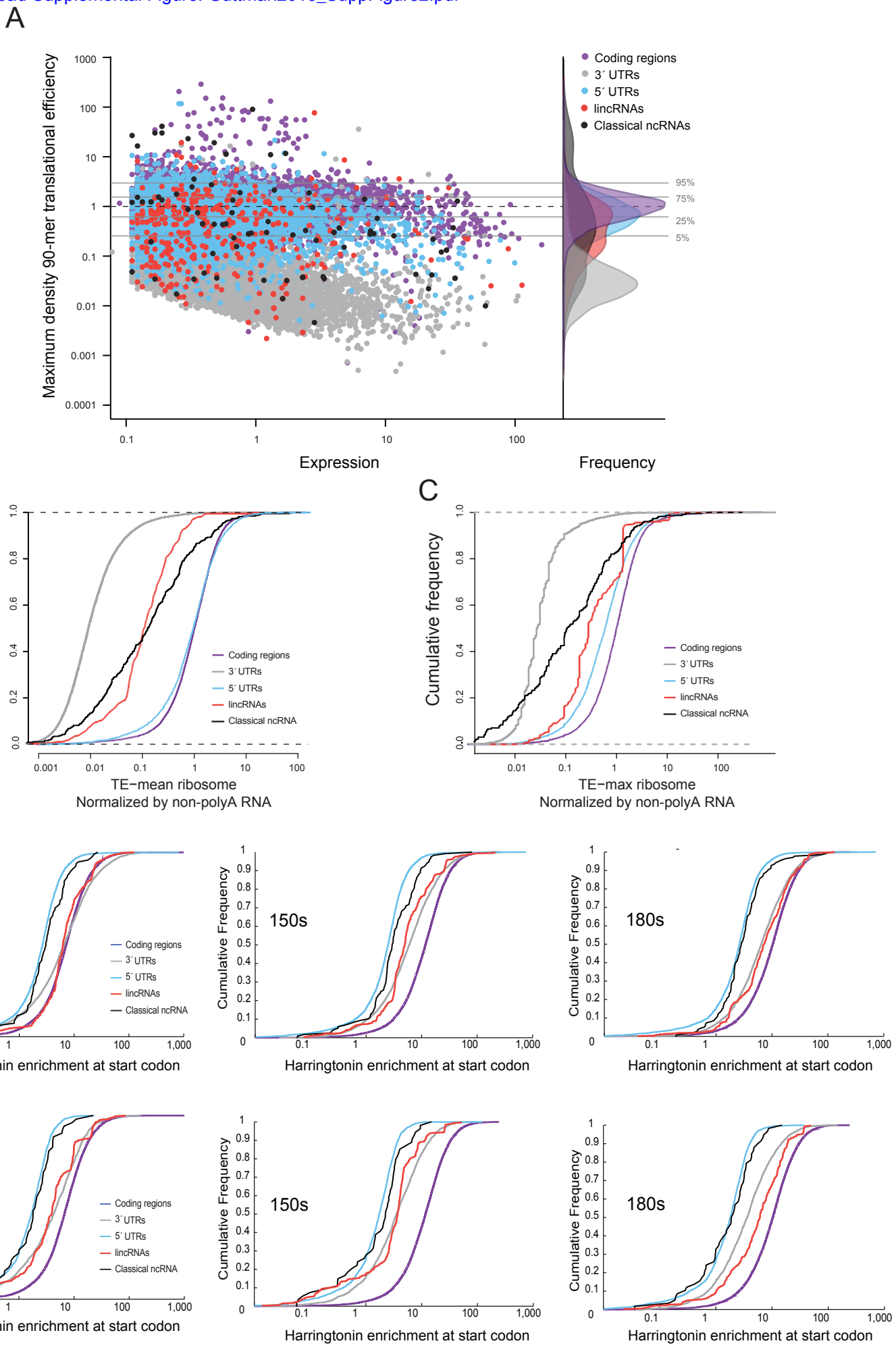

Supplemental Figure3

Click here to download Supplemental Figure: Guttman2013_SuppFigure3.pdf

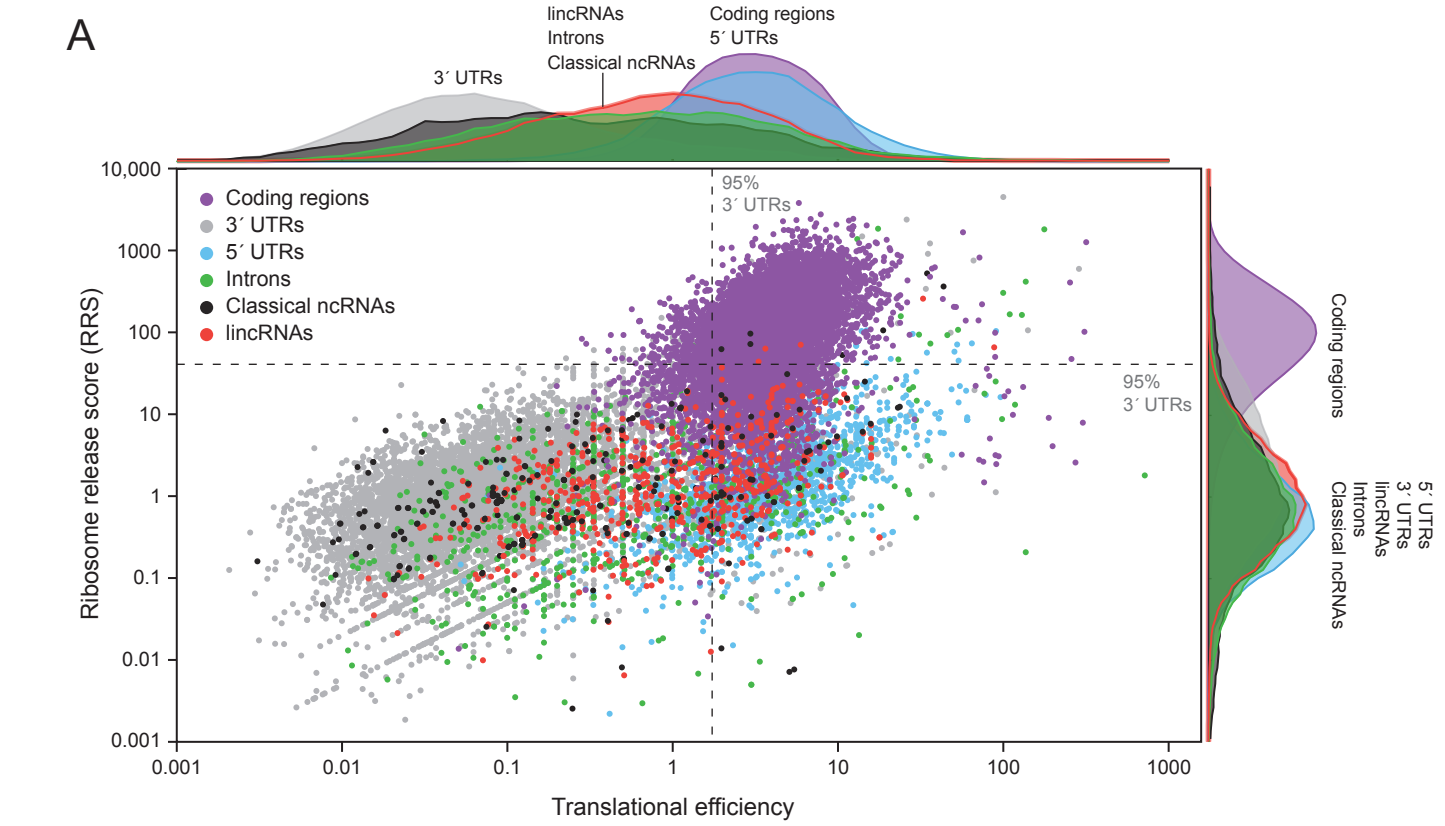

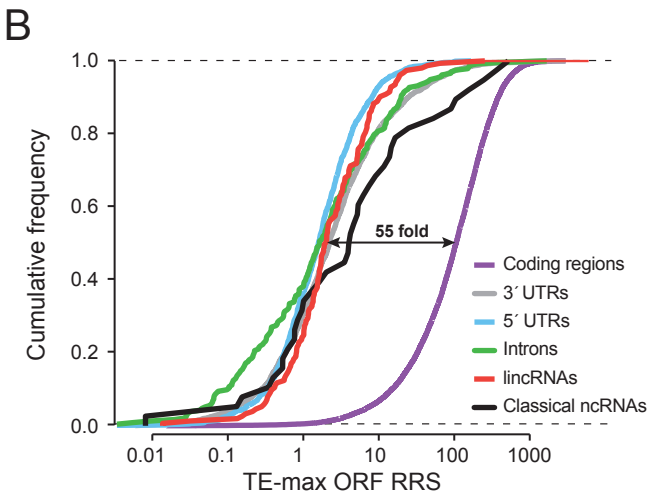

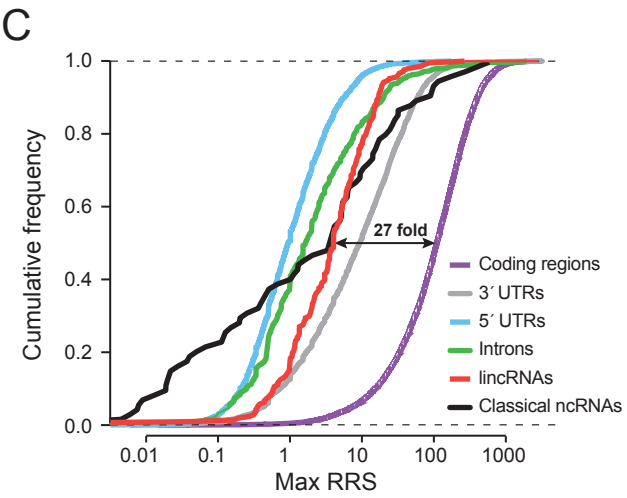

Supplemental Figure4

Click here to download Supplemental Figure: Guttman2013_SuppFigure4.pdf